

Interaction of red blood cells with arrays of laser-induced cavitation bubbles

Pedro A. Quinto-Su

Division of Physics and Applied
Physics, SPMS
Nanyang Technological
University, Singapore

Rory Dijkink

Physics of Fluids, Faculty of
Science, University of Twente,
The Netherlands

Firdaus Prabowo

Division of Physics and Applied
Physics, SPMS
Nanyang Technological
University, Singapore

Karthigayan Gunalan

Nanyang Technological
University, Singapore

Peter Rainer Preiser

Nanyang Technological
University, Singapore

Claus-Dieter Ohl

Division of Physics and Applied
Physics, SPMS
Nanyang Technological
University, Singapore

ABSTRACT

We use a spatial light modulator (SLM) to simultaneously create several laser-induced cavitation bubbles. The geometry of the bubble array results in different flow patterns during the expansion and collapse of the bubbles. Hence, the induced shear stresses that affect cells are also modified by the geometry. The events are imaged using strobe photography and high speed cameras. In particular we study the deformability of red blood cells due to the shear stresses, since RBC deformability is a potential indicator for several diseases including malaria [1].

INTRODUCTION

Laser-induced cavitation bubbles and the flow resulting from cavitation events have been used to lyse, porate and perform microsurgery in cells [2, 3, 4]. Usually, a laser pulse is focused through a microscope objective into the sample to create a single cavitation bubble. The bubble expands and collapses within a few microseconds and can induce flows with speeds of several m/s. The shear produced by the rapid bubble dynamics has been used to interact with cells. However, since the flow induced by the expansion and collapse of a single bubble is radial symmetric, there is no preferred direction in which the effects of the flow can be tuned to have a desired effect on cells. This problem can be overcome by using more than one cavitation bubble to create more complex and asymmetric flows.

Recently we demonstrated the use of an SLM to create arbitrary arrays of bubbles [5]. These arrays of laser induced cavitation bubbles offer the possibility of breaking the symmetry of the induced flow and the creation of jets. In this way it is possible to have spatial regions with maximum

induced shears, while on other locations the effect would be very small.

EXPERIMENTAL SET UP

A Nd:YAG laser generates a single pulse at 532 nm with a duration of 6ns (Figure 1). It propagates through a half wave plate to rotate the polarization and then it goes through a telescope formed by lenses L1 and L2 to expand the beam to fill the display of the SLM. A digital hologram is projected on the SLM to create multiple foci's. The pattern on the SLM imparts the phases needed to recreate the desired pattern at the focal plane of the microscope objective. The pattern is focused inside a very thin microchannel filled with ink which absorbs the laser light, so that at each laser foci a cavitation bubble is generated.

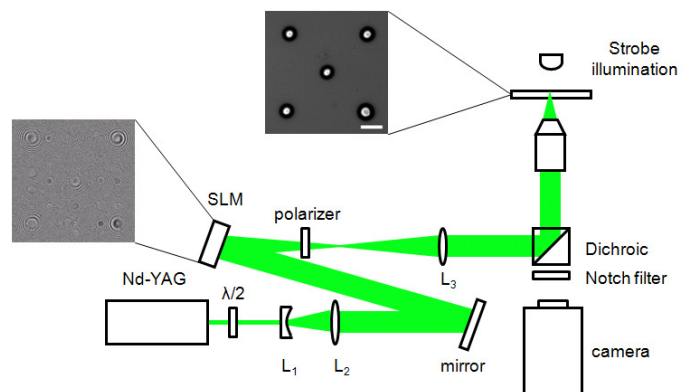


Figure 1: Experimental setup.

On the upper-left inset in Figure 1 (above the SLM) we show the hologram used to create ‘five on a dice’ pattern shown on the second inset. The events are illuminated with a homebuilt strobe consisting of a high power light emitting diode (LED) or fluorescent light excited by a pair of green pump lasers which is collected into an optical fiber (not shown in Figure 1).

In Figure 2 we show the images of a shock wave generated by a single laser-induced cavitation bubble, the shock wave is imaged at two different positions with a couple of flashes from the laser strobe with a temporal delay of 50ns. This shows the kind of spatial and temporal resolution that we can achieve with our system. In addition, we want to study the effect that shock waves have on cells within a few ns after the passing of the shock wave.

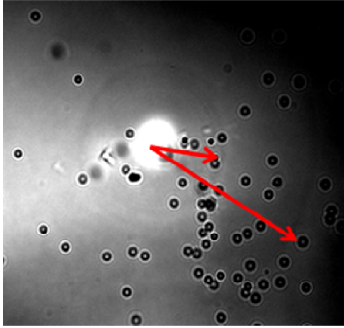


Figure 2: Shockwave generated by a single laser-induced cavitation bubble, the image is illuminated 2 times with a delay of 50ns between the flashes. The arrows show the shock wave at two different positions as it propagates. DOUBLE shutter....

Figure 3 shows an array of 9 bubbles imaged at $1.2\mu\text{s}$ after their creation. The interaction between four bubbles and red blood cells is shown on Figure 4 during the expansion and collapse of the bubble array.

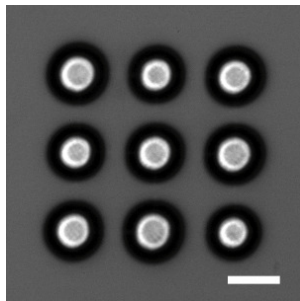


Figure 3: Array of 9 expanding bubbles ($E=44\ \mu\text{J}$) imaged at $1.2\mu\text{s}$ after generation. The length of the scale bar is $100\ \mu\text{m}$.

Cells: Red blood cells from a healthy donor (RBCs) are placed inside a thin microchannel which consists of a couple of microscope coverslips separated by spacers with a height of $15\mu\text{m}$, this geometry prevents the cells from lifting out of focus during their interaction with the flow induced by the bubbles.

RESULTS

We can create arbitrary arrays of bubble clusters as shown in Figure 3. A specific example of interaction of cells with an array of laser-induced cavitation bubbles is shown on Figure 4,

where four cavitation bubbles are created. The bubbles interact with red blood cell. On (a) it is during the expansion and (b) shows the collapse of the bubbles and several deformed RBCs.

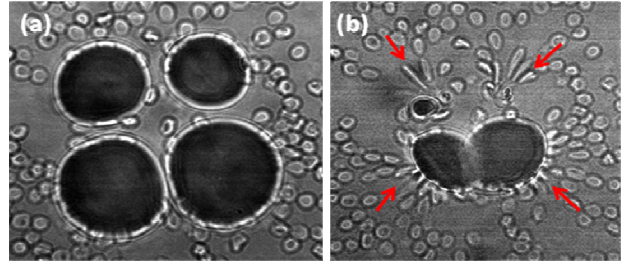


Figure 4: Array of 4 bubbles interacting with red blood cells. (a) Expansion of the bubbles. (b) Collapse of the array and deformation of the cells.

Several of the deformed RBCs on Figure 4(b) have an elongated ‘tear drop’ shape, which is a result of the different shear stresses that act along the cell surface. In order to understand this deformation we look at the flow induced by a single cavitation bubble. We assume that the geometry of the thin microchannel is essentially two-dimensional. Since the height of the channel is smaller than the maximum bubble radius.

For short times the flow in the center of the channel is not affected by the no-slip boundary conditions at the bottom and at the top of the channel, or in other words, vorticity had not time to diffuse yet into the center of the channel. The liquid in the middle can be modeled as potential flow with a velocity profile that scales as $1/r$ where r is the distance from the center of the bubble.

This could explain why the different points along a RBC are sheared at different rates. In order to get some insight into the RBC observed shapes during the collapse of the bubbles (like in Figure 4b) we look at how circular fluid particles are mapped during the collapse of a single bubble, assuming potential flow. The results are shown in Figures 5a and b, where we see circles with a diameter of $5\ \mu\text{m}$ are transformed into elongated shapes similar to the ones that we observe on figure 4b. In Figures 5a and 5b the large dotted circle represents the bubble radius at the start of the simulation that considers the collapse of that initial bubble. The initial position of the $5\ \mu\text{m}$ circles is shown in the figures (left side of the bubble) along with the final position of the ‘deformed circles’ after the collapse of the bubble. The final shapes resemble those seen on Figure 4b.

However, this simple model doesn’t explain the deformation of the RBCs into ‘tear drop shapes’ during the expansion of the bubbles. Figure 6 shows an example of some RBC’s being elongated during the expansion of two bubbles. On the upper left corner of Figure 6 the cells are shown prior to the arrival of the laser pulse, the frame on the upper right shows the expanding bubble at $2\ \mu\text{s}$ after the arrival of the laser pulse.

We can see that two cells (marked by an arrow) are being elongated. On the next frame taken $5\mu\text{s}$ after the laser pulse we see that the cells have been stretched further. And finally on the last frame taken after a few seconds of the bubble collapse we observe that the cells have recovered their original shape.

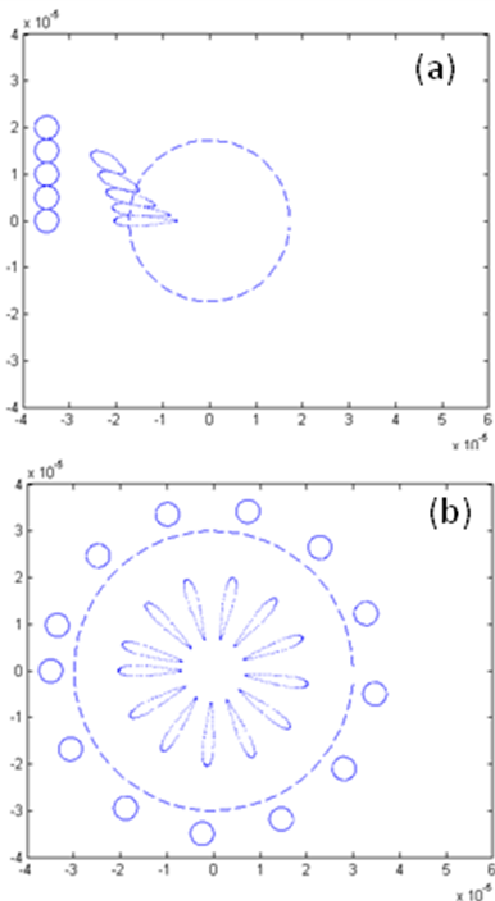


Figure 5: (a) Top and (b) bottom. The dotted circle represents the bubble radius at the start of the simulation, the smaller circles show the initial state at that time and then after the bubble collapses the new elongated shapes are shown. The separation between the x- and y-ticks is $10 \mu\text{m}$.

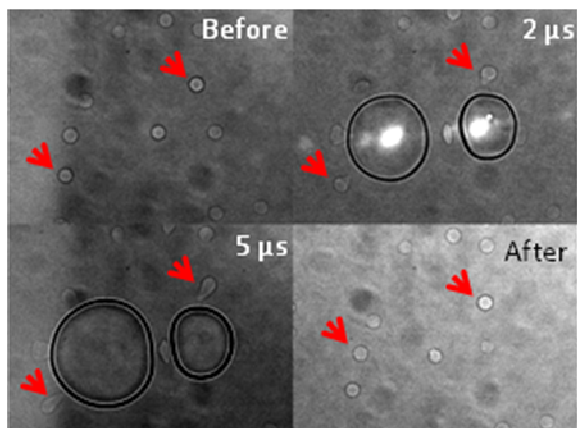


Figure 6: Upper left corner: RBCs before the arrival of the laser pulse. Upper right and lower left corner: stretching of the marked RBCs during the expansion of the bubbles (2 and $5 \mu\text{s}$). Lower right corner: cell shape recovery a few seconds after the collapse of the bubble.

The elongation of the cells (tear drop shape) during the expansion of the cavitation bubbles can't be explained by the potential flow model. Since the velocity scales as $1/r$ which means that points along the cell closer to the center of the bubble should be experiencing higher shear, while the points on the cell farther away from the bubble center should be under lower velocity flow. Hence, there should be no elongation of the cell, but some folding or compression. To explain this effect, we need to consider the change in velocity of the flow as a function of height going from the zero velocity at the surface of the microchannel to the maximum flow speed at the center.

CONCLUSION AND OUTLOOK

Using double shutter strobe photography with temporal resolution of a few ns, we can observe the interaction between systems of bubbles and cells. We see noticeable deformation of RBCs during the collapse (Figure 4b) and expansion (Figure 6) of the bubbles. Using this technique, we are currently studying and quantifying the deformation of the cells as they interact with bubble arrays. We plan to quantify the deformation by measuring the time it takes the cells to recover their original shape after being deformed by laser-induced cavitation bubbles.

ACKNOWLEDGMENTS

MOE and NTU, Singapore (T208A1238, R G39/07), and NWO, The Netherlands.

REFERENCES

- [1] Y.Park, M. Diez-Silva, G. Popescu, G. Lykotrafitis, W. Choi, M. S. Feld and S. Suresh, "Refractive index maps and membrane dynamics of human red blood cells parasitized by *Plasmodium falciparum*" *PNAS* **105**, 13730-13735 (2008).
- [2] K.R. Rau, P.A. Quinto-Su, A.N. Hellman, V. Venugopalan, "Pulsed laser microbeam-induced cell lysis: Time-resolved imaging and analysis of hydrodynamic effects," *Biophys. J.* **91**, 317-329 (2006).
- [3] Dijkink, S. Le Gac, E. Nijhuis, A. van de Berg, I. Vermes, A. Poot, C.D. Ohl, "Controlled cavitation-cell interaction: trans-membrane transport and viability studies," *Phys. Med. Bio.* **53**, 375-390 (2008).
- [4] S. Le Gac, E. Zwaan, A. van den Berg, C.D. Ohl, "Sonoporation of suspension cells with a single cavitation bubble in a microfluidic confinement," *Lab Chip* **7**, 1666-1672 (2007).
- [5] P. A. Quinto-Su, V. Venugopalan and C.-D. Ohl, "Generation of laser-induced cavitation bubbles with a digital hologram" *Opt. Exp.* **16**, 18964-18969 (2008).